

# Vibrational Coherences and Relaxation in the High-Spin State of Aqueous $[\text{Fe}^{\text{II}}(\text{bpy})_3]^{2+}$ \*\*

Cristina Consani, Mirabelle Prémont-Schwarz, Amal ElNahhas, Christian Bressler, Frank van Mourik, Andrea Cannizzo, and Majed Chergui\*

In memory of Vladilen Stepanovich Letokhov

Iron(II)-based molecular complexes have been a subject of intense study since the discovery of light-induced excited-state spin trapping (LIESST).<sup>[1]</sup> In this process, excitation of the singlet low-spin (LS) ground state with UV or visible light to the metal-to-ligand charge-transfer states ( $^1\text{MLCT}$ ) or to the lower-lying singlet and triplet ligand-field ( $^1\text{LF}$ , also called metal-centered) states (see Figure S1 in the Supporting Information) leads to population of the lowest high-spin (HS) excited quintet  $^5\text{T}_2$  state by nonradiative relaxation.<sup>[2]</sup> We recently characterized the relaxation cascade from the initially excited  $^1\text{MLCT}$  state to the lowest excited quintet state of aqueous  $[\text{Fe}^{\text{II}}(\text{bpy})_3]^{2+}$  upon 400 nm excitation using ultrafast optical and X-ray spectroscopic techniques<sup>[3,4]</sup> and showed that it is a three-step  $^1\text{MLCT}$ – $^3\text{MLCT}$ – $^5\text{T}_2$  process that takes place in approximately 150 fs and bypasses the intermediate  $^1\text{LF}$  states.

Since the minima of the  $^3\text{MLCT}$  and  $^5\text{T}_2$  states lie approximately 1.3 eV<sup>[3,5]</sup> apart, the above mechanism implies that the energy difference is stored as vibrational energy in the  $^5\text{T}_2$  state. Given that a large number of  $\text{Fe}^{\text{II}}$  complexes can undergo LS-to-HS transitions (and vice versa) under the effect of temperature,<sup>[6]</sup> the issue of vibrational energy storage and relaxation in the quintet state is important. It was recently addressed by McCusker and co-workers using femtosecond stimulated Raman scattering of  $[\text{Fe}^{\text{II}}(\text{tren}(\text{py})_3)]^{2+}$  in acetonitrile ( $\text{tren}(\text{py})_3 = \text{tris}(2\text{-pyridylmethyliminoethyl})\text{amine}$ ),<sup>[7]</sup> who reported a bimodal time evolution of the high-frequency C–N stretching mode with time constants of  $(190 \pm 50)$  fs and  $(10 \pm 3)$  ps.<sup>[7]</sup> The latter was attributed to vibrational cooling, while the former was associated with the structural change from LS to HS. Wolf et al.<sup>[8]</sup> reported on a sub-picosecond IR

study of  $[\text{Fe}^{\text{II}}(\text{btpa})]^{2+}$  and  $[\text{Fe}^{\text{II}}(\text{b}(\text{bdpa}))]^{2+}$  in the 1000–1100  $\text{cm}^{-1}$  region ( $\text{b}(\text{btpa}) = \text{bis}(N,N,N',N'\text{-tetrakis}(2\text{-pyridylmethyl})\text{-}6,6'\text{-bis}(\text{aminoethyl})\text{-}2,2'\text{-bipyridine})$ ;  $\text{bdpa} = N,N'\text{-bis}(\text{benzyl})\text{-}N,N'\text{-bis}(2\text{-pyridylmethyl})\text{-}6,6'\text{-bis}(\text{aminoethyl})\text{-}2,2'\text{-bipyridine}$ ), and found relaxation times near 10 ps in both cases. The quintet states of  $\text{Fe}^{\text{II}}$  complexes absorb in the UV region near 300 nm,<sup>[2,7,9]</sup> and herein we use visible pump/UV probe spectroscopy with a resolution of approximately 130 fs to monitor the vibrational relaxation in the quintet state of aqueous  $[\text{Fe}^{\text{II}}(\text{bpy})_3]^{2+}$  ( $\text{bpy} = 2,2'\text{-bipyridine}$ ). We report on the observation of vibrational wave packets for the first time in the HS state of this class of complexes, and we also determine the vibrational relaxation times.

Figure 1 shows UV transient absorption spectra for different time delays, which are extracted from the 2D time–wavelength plots recorded with the UV continuum probe (see Figure S2 in the Supporting Information). The

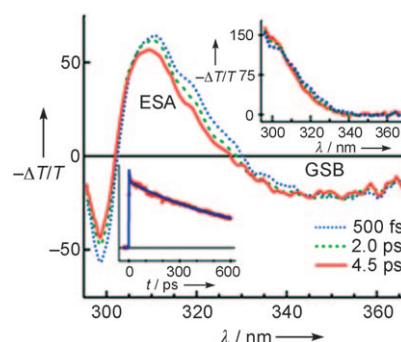


**Figure 1.** UV transient absorption spectra at different time delays upon excitation of aqueous  $[\text{Fe}^{\text{II}}(\text{bpy})_3]^{2+}$  at 530 nm. The bottom inset shows a long-time kinetic trace recorded at 315 nm. The top inset shows excited-state absorption spectra at different time delays, obtained by subtracting the ground-state spectrum from the transient spectra (see Figure S2 in the Supporting Information). The resulting curve corresponds to the absorption spectrum of the high-spin quintet state, similar to that reported in the literature for  $\text{Fe}^{\text{II}}$  complexes with a HS ground state.<sup>[7]</sup> GSB = ground-state bleaching.

positive region between 300 and approximately 330 nm corresponds to an excited-state absorption (ESA), while elsewhere in the spectrum a bleach signal is dominant, which matches quite well to the ground-state absorption spectrum above 350 nm (see Figure S3 in the Supporting Information). The ESA is due to the quintet state, as evidenced by its decay

[\*] C. Consani, M. Prémont-Schwarz,<sup>[†]</sup> A. ElNahhas, Prof. Dr. C. Bressler, Dr. F. van Mourik, Dr. A. Cannizzo, Prof. Dr. M. Chergui  
Ecole Polytechnique Fédérale de Lausanne (EPFL)  
Laboratoire de Spectroscopie Ultrarapide (LSU)  
ISIC, Faculté des Sciences de Base, BSP  
1015 Lausanne-Dorigny (Switzerland)  
Fax: (+41) 21-693-0422  
E-mail: majed.chergui@epfl.ch

[†] Current address: Max-Born Institute  
Max-Born-Strasse 2A, 12489 Berlin (Germany)

[\*\*] This work was funded by the Swiss NSF via contracts 620-066145, 200021-107956 and 200021-105239. We are grateful to Prof. A. Hauser (Geneva) for useful discussions.  $\text{bpy} = 2,2'\text{-bipyridine}$ .

Supporting information for this article is available on the WWW under <http://dx.doi.org/10.1002/anie.200902728>.

time of 650–700 ps (see bottom inset, Figure 1), but the kinetics also exhibits a short component of 2–3 ps. By normalizing the absorption spectrum to the TA spectrum above 350 nm (Figure S3 in the Supporting Information), we could retrieve the absorption spectrum of the quintet state at different time delays (top inset, Figure 1). The long-time spectra agree with those of HS Fe<sup>II</sup> complexes.<sup>[7]</sup>

We investigated the early time behavior of the system by recording kinetic traces between 300 and 360 nm (Figure 2). The bleach traces are characterized by a fast drop at time

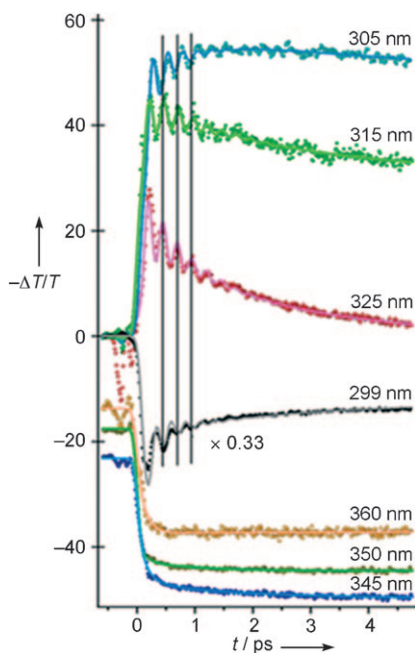


**Figure 2.** Kinetic traces at different probe wavelengths (extracted from Figure S2 in the Supporting Information) covering the ESA (305, 315, and 325 nm) and the bleach regions (299, 345, 350, and 360 nm). Solid lines represent the fits using Equations (1) and (2) (see the Supporting Information for details) and the parameters of Table S1 in the Supporting Information. The vertical lines show the phase shift of approximately  $\pi$  of the oscillations between the blue-most and the red-most probe wavelengths in the ESA region. For the sake of clarity, time traces at  $\lambda > 340$  nm have been vertically shifted, and the one at 299 nm is scaled to 1/3.

zero, and (for the 350 and 345 nm traces) a subsequent additional decrease (ca. 20 %) on a time scale of 1–3 ps, which suggests a contribution of the ESA to these bleach traces (top inset, Figure 1). The traces in the ESA region are all characterized by a fast rise, a subsequent oscillatory pattern, and a longer decaying component. The latter pattern is also found in the blue-most bleach trace at 299 nm, as this region contains a strong ESA contribution (Figure 1 and Figure S3 in the Supporting Information). The oscillations at the blue and red edges of the ESA (299 and 325 nm) exhibit a phase shift close to  $\pi$  (vertical lines, Figure 2), which is typical of a wave packet oscillating between the turning points of the potential surface on which it evolves.<sup>[10]</sup> The oscillation period of 254 fs is independent of probe wavelength. To fit the kinetic traces, we used our prior knowledge about the system: 1) the 130 fs

lifetime of the <sup>3</sup>MLCT state;<sup>[3]</sup> 2) the MLCT ([Fe<sup>III</sup>(bpy)<sub>2</sub>]<sup>2+</sup>) absorption, which has bands of increasing intensity down to 300 nm;<sup>[11]</sup> 3) the quintet-state lifetime of 650 ps<sup>[9]</sup> and its absorption spectrum (Figure 1 and reference [7]).

The kinetic trace at 360 nm is fitted at early times by a short-lived (130 fs) positive contribution arising from the ESA by the MLCT states and by a promptly rising (within the cross-correlation) bleach (negative) component recovering on a time constant of 650 ps (Figure 2). These components are in agreement with those previously reported for the signal at 370 nm.<sup>[3]</sup> However, as the probe is progressively tuned to the blue, in addition to the  $\tau_{\text{MLCT}} \approx 130$  fs ESA and 650 ps ground-state bleaching (GSB) components, more components are needed to obtain satisfactory fits. The 350 nm trace exhibits a positive component with  $\tau_1 = (1.1 \pm 0.17)$  ps, while the 345 nm trace exhibits the 1.1 ps component and an additional positive component with  $\tau_2 = (3.4 \pm 1.2)$  ps. As mentioned above, at these wavelengths the spectra also contain a contribution of the ESA (Figure 1 and Figure S3 in the Supporting Information). It is thus reasonable to assume that the additional time components stem from the ESA, as supported by the fits discussed below. In fact, both of these components are found as decaying contributions in the red-most part of the ESA region. Moreover, in the ESA region, the rise time of the signal is 180–190 fs (larger than the cross-correlation of approximately 130 fs, see Figure S4 in the Supporting Information), which is consistent with the presence of the approximately 130 fs MLCT ESA convoluted with the approximately 130 fs Gaussian instrument response function (IRF) of our setup. The time traces are fitted by Equation (1):

$$\Delta OD(t) = [Q(t) + GSB(t) + T(t)] \otimes \text{IRF}(t) \quad (1)$$

where  $Q(t)$  represents the HS state dynamics,  $GSB(t)$  is the ground-state bleach signal, and  $QT(t)$  is the contribution of the short-lived MLCT state absorption (for more details, see the Supporting Information). The quintet-state contribution (the derivation of this expression is given in the Supporting Information) is written as in Equation (2):

$$Q(t) = \sum_{i=1}^3 A_i u(t) (e^{-t/\tau_i} - e^{-t/\tau_{\text{MLCT}}}) + A_{\text{osc}} u(t) (\sin(\omega t + \varphi) e^{-t/\tau_d} - \sin \varphi e^{-t/\tau_{\text{MLCT}}}) \quad (2)$$

where  $u(t)$  is a step function,  $\tau_1$  and  $\tau_2$  represent the decay constants extracted above,  $\tau_3 = 650$  ps is the relaxation time from the quintet to the ground state,<sup>[9]</sup> and  $\tau_{\text{MLCT}} = 130$  fs is the rise time associated with population from the MLCT state. These four time constants are wavelength-independent, and Table S1 in the Supporting Information gives the fit parameters: the damping time of the oscillations ( $\tau_d$ ) and their amplitude ( $A_{\text{osc}}$ ). Finally, the pre exponential factors ( $A_i$ ) are plotted in Figure S5 in the Supporting Information as a function of probe wavelength.

The fit results show good agreement with the experimental traces over the whole spectral range (Figure 2). The wavelength dependence of  $\tau_d$  is not surprising since the damping of the oscillations is not only due to the dephasing time of the wave packet but is also determined by the probe

window in configuration space, which depends on the probe wavelength and its spectral width and on the relative curvatures of the initial and final potential surfaces.<sup>[12]</sup> In this respect, the largest value is found at 315 nm, which agrees with the  $\pi$  phase shift around 310 nm. The pre-exponential factors confirm the consistency of the fit, as  $A_3$  (650 ps component, Figure S5c in the Supporting Information) maps out fairly well the HS absorption (Figure 1), and the  $A_T$  (130 fs) component (Figure S5d and Eq. (S8) in the Supporting Information) maps the MLCT absorption.<sup>[11]</sup> The fact that the pre-exponential factors in Figures S5c and S5d in the Supporting Information have rather similar values also reflects the rather similar absorption coefficients of the HS<sup>[7]</sup> and MLCT absorptions.<sup>[11]</sup> The 3.4 ps component also partly maps the quintet-state absorption, but there is a change of sign around 305 nm. This is due to the fact that on this time scale, the quintet-state absorption band narrows owing to cooling, and its maximum increases, as evidenced by the isosbestic point around 305 nm in Figure 1 (top inset). A change of sign also occurs for the 1.1 ps component (Figure S5a in the Supporting Information) at longer wavelengths, and even though a narrowing of the quintet absorption band may be observed on this time scale (not shown here), it is difficult to distinguish owing to the superposition of the oscillatory response. These observations indicate that vibrational cooling in the HS state occurs in a bimodal regime.

Although the absolute phase of the oscillations cannot be deduced owing to cross-phase modulation (Table S1 in the Supporting Information), it is clear that the vibrational coherences occur on the HS surface because they only appear in the ESA region, and they are absent from the GSB traces above 325 nm and in the visible region.<sup>[3]</sup> We can thus rule out an impulsive Raman excitation of vibrational wave packets in the ground state. The reaction coordinate of the photoexcited LS–HS spin-change process is the Fe–N bond elongation,<sup>[4]</sup> but the observed oscillation wavenumber (130 cm<sup>−1</sup>) does not correspond to the Fe–N stretching mode, which is around 400 cm<sup>−1</sup> (ca. 80 fs) in the ground state and 220 cm<sup>−1</sup> (ca. 150 fs) in the HS state for nearly all Fe<sup>II</sup>-based polypyridine complexes.<sup>[13]</sup> The observed wave packet is therefore not directly excited by the laser pulse but by the higher-frequency Fe–N stretching mode. Indeed, an ultrafast elongation of the Fe–N bonds implies an impulsive change of N–Fe–N angle from LS to HS, which most probably excites bending modes. Given the difference in periods of the stretching mode (ca. 150 fs) relative to the observed oscillation (254 fs), the wave packet consists of a coherent superposition of barely two to three vibrational levels. The indirect excitation of wave packets of low-frequency modes by laser-excited (not necessarily in the form of wave packets) higher frequency ones is rather common in many systems, including metalloproteins<sup>[14]</sup> and organic molecules.<sup>[15]</sup> In our case, the invariance of the oscillation period with probe wavelength suggests that the wave packet is created near the minimum of the surface on which it evolves.

Raman studies of the ground state of [Fe<sup>II</sup>(bpy)<sub>3</sub>]<sup>2+</sup> detected a lowest vibrational mode of the molecule at 146 cm<sup>−1</sup>.<sup>[16]</sup> More recently, DFT calculations predicted a mode at 128 cm<sup>−1</sup> in [Fe<sup>II</sup>(bpy)<sub>3</sub>]<sup>2+</sup><sup>[17]</sup> and at 133 cm<sup>−1</sup> for the

HS state of [Fe<sup>II</sup>(phen)<sub>2</sub>(NCS)<sub>2</sub>]<sup>2+</sup> (phen = 1,10-phenanthroline),<sup>[18]</sup> while in the latter study, a Raman band at 131 cm<sup>−1</sup> was also reported. The 128 cm<sup>−1</sup> frequency has been attributed to a combination of chelate-ring modes, benzene cycle bending modes, and N–Fe–N bending modes.<sup>[17]</sup>

The damping times of the wave packet (Table S1 in the Supporting Information) represent a lower limit of its dephasing time, since, as mentioned above, they also depend on the probe window. The dephasing causes the coherent (oscillatory) wave-packet dynamics to turn into an incoherent kinetic regime (exponential). Given that the largest dephasing time we found is approximately 800 fs, it is tempting to attribute the 1.1 ps decay component to the dephasing of the 130 cm<sup>−1</sup> mode. Concerning the 3.4 ps decay, we attribute it to the relaxation time of the (incoherently) excited Fe–N stretch mode in the quintet state. The 3.4 ps relaxation time reported herein is significantly smaller than the approximately 10 ps reported in the femtosecond stimulated Raman and IR experiments,<sup>[7,8]</sup> and this difference is clearly due to the fact that the latter studies deal with different iron complexes and with higher frequency modes. In this last respect, our recent ultrafast fluorescence studies of [Ru<sup>II</sup>(bpy)<sub>3</sub>]<sup>2+</sup><sup>[19]</sup> and [Fe<sup>II</sup>(bpy)<sub>3</sub>]<sup>2+</sup><sup>[3]</sup> showed that the <sup>1,3</sup>MLCT emissions are vibrationally cold, at least as far as high-frequency modes are concerned, even at very early times (less than 100 fs). This would imply that upon crossing into the quintet state, only the Fe–N stretch and the N–Fe–N chelate-ring modes are excited, which are responsible for the bimodal relaxation regime.

We have reported on the appearance of vibrational wave packets in the HS state of an Fe<sup>II</sup> complex for the first time. The ability to perform time-domain studies of the vibrational dynamics opens the possibility to map out the modes involved in the ultrafast spin changes in a large class of metal-based molecular complexes.

## Experimental Section

The experimental setup is described in detail in the Supporting Information. Briefly, an aqueous solution of 28 mM [Fe<sup>II</sup>(bpy)<sub>3</sub>]<sup>2+</sup> is flown in a 100  $\mu$ m thick UV-grade flow cell and excited by a 50 fs pulse at 530 nm. The dynamics are probed by a broadband UV probe pulse (ca. 70 fs). The cross-correlation of approximately 130 fs was determined on the pure water solvent.

Received: May 21, 2009

Published online: August 28, 2009

**Keywords:** iron · spin crossover · time-resolved spectroscopy · ultrafast dynamics · vibrational relaxation

[1] P. Gutlich, H. A. Goodwin, *Top. Curr. Chem.* **2004**, 233, 1.

[2] A. Hauser, *Top. Curr. Chem.* **2004**, 234, 155.

[3] W. Gawelda, A. Cannizzo, V. T. Pham, F. van Mourik, C. Bressler, M. Chergui, *J. Am. Chem. Soc.* **2007**, 129, 8199.

[4] C. Bressler, C. Milne, V. T. Pham, A. ElNahhas, R. M. van der Veen, W. Gawelda, S. Johnson, P. Beaud, D. Grolimund, M. Kaiser, C. N. Borca, G. Ingold, R. Abela, M. Chergui, *Science* **2009**, 323, 489.

- [5] L. M. Lawson Daku, A. Vargas, A. Hauser, A. Fouqueau, M. E. Casida, *ChemPhysChem* **2005**, *6*, 1393.
- [6] P. Gütllich, Y. Garcia, H. A. Goodwin, *Chem. Soc. Rev.* **2000**, *29*, 419.
- [7] A. L. Smeigh, M. Creelman, R. A. Mathies, J. K. McCusker, *J. Am. Chem. Soc.* **2008**, *130*, 14105.
- [8] M. M. N. Wolf, R. Gross, C. Schumann, J. A. Wolny, V. Schunemann, A. Dossing, H. Paulsen, J. J. McGarvey, R. Diller, *Phys. Chem. Chem. Phys.* **2008**, *10*, 4264.
- [9] J. K. McCusker, K. N. Walda, R. C. Dunn, J. D. Simon, D. Magde, D. N. Hendrickson, *J. Am. Chem. Soc.* **1992**, *114*, 6919.
- [10] M. Guhr, M. Bargheer, M. Fushitani, T. Kiljunen, N. Schwentner, *Phys. Chem. Chem. Phys.* **2007**, *9*, 779.
- [11] P. S. Braterman, J. I. Song, R. D. Peacock, *Inorg. Chem.* **1992**, *31*, 555.
- [12] C. Jeannin, M. T. Porrella-Oberli, S. Jimenez, F. Vigliotti, B. Lang, M. Chergui, *Chem. Phys. Lett.* **2000**, *316*, 51.
- [13] J. P. Tuchagues, A. Bousseksou, G. Molnar, J. J. McGarvey, F. Varret, *Top. Curr. Chem.* **2004**, *235*, 85.
- [14] F. Rosca, A. T. N. Kumar, D. Ionascu, X. Ye, A. A. Demidov, T. Sjödin, D. Wharton, D. Barrick, S. G. Sligar, T. Yonetani, P. M. Champion, *J. Phys. Chem. A* **2002**, *106*, 3540.
- [15] G. Zgrablic, S. Haacke, M. Chergui, *Chem. Phys.* **2007**, *338*, 168.
- [16] R. J. H. Clark, P. C. Turtle, D. P. Strommen, B. Streusand, J. Kincaid, K. Nakamoto, *Inorg. Chem.* **1977**, *16*, 84.
- [17] B. D. Alexander, T. J. Dines, R. W. Longhurst, *Chem. Phys.* **2008**, *352*, 19.
- [18] K. L. Ronayne, H. Paulsen, A. Hofer, A. C. Dennis, J. A. Wolny, A. I. Chumakov, V. Schunemann, H. Winkler, H. Spiering, A. Bousseksou, P. Gütllich, A. X. Trautwein, J. J. McGarvey, *Phys. Chem. Chem. Phys.* **2006**, *8*, 4685.
- [19] A. Cannizzo, F. van Mourik, W. Gawelda, G. Zgrablic, C. Bressler, M. Chergui, *Angew. Chem.* **2006**, *118*, 3246; *Angew. Chem. Int. Ed.* **2006**, *45*, 3174.